13662–13673 *Nucleic Acids Research, 2014, Vol. 42, No. 22* *Published online 20 November 2014*
doi: 10.1093/nar/gku1226

Identification by high-throughput imaging of the histone methyltransferase EHMT2 as an epigenetic regulator of VEGFA alternative splicing

Maayan Salton*, Ty C. Voss and Tom Misteli*

National Cancer Institute, NIH, Bethesda, MD 20892, USA

Received July 30, 2014; Revised October 22, 2014; Accepted November 09, 2014

ABSTRACT

Recent evidence points to a role of chromatin in regulation of alternative pre-mRNA splicing (AS). In order to identify novel chromatin regulators of AS, we screened an RNAi library of chromatin proteins using a cell-based high-throughput *in vivo* assay. We identified a set of chromatin proteins that regulate AS. Using simultaneous genome-wide expression and AS analysis, we demonstrate distinct and non-overlapping functions of these chromatin modifiers on transcription and AS. Detailed mechanistic characterization of one dual function chromatin modifier, the H3K9 methyltransferase EHMT2 (G9a), identified VEGFA as a major chromatin-mediated AS target. Silencing of EHMT2, or its heterodimer partner EHMT1, affects AS by promoting exclusion of VEGFA exon 6a, but does not alter total VEGFA mRNA levels. The epigenetic regulatory mechanism of AS by EHMT2 involves an adaptor system consisting of the chromatin modulator HP1γ, which binds methylated H3K9 and recruits splicing regulator SRSF1. The epigenetic regulation of VEGFA is physiologically relevant since EHMT2 is transcriptionally induced in response to hypoxia and triggers concomitant changes in AS of VEGFA. These results characterize a novel epigenetic regulatory mechanism of AS and they demonstrate separate roles of epigenetic modifiers in transcription and alternative splicing.

INTRODUCTION

Newly synthesized precursor mRNAs (pre-mRNA) undergo extensive co-transcriptional and post-transcriptional processing. Of particular importance is pre-mRNA splicing, during which non-coding intron sequences are removed from the nascent RNA. Pre-mRNA splicing is thought to occur largely co-transcriptionally and physical interaction of the transcription and RNA splicing machinery has been reported (1–3). While the main purpose of RNA splicing is the removal of non-coding intron regions and the linear joining of coding exons, they may also be joined in a combinatorial fashion in a process referred to as alternative splicing (AS). This process is physiologically relevant as it gives rise to multiple protein isoforms from one pre-mRNA molecule, thereby contributing to proteomic diversity (4). Novel high-throughput sequencing technology has recently revealed that more than 90% of human genes undergo AS (5) and AS is recognized as a key regulatory mechanism in differentiation and tissue-specific gene expression (6). Alternative splice site selection appears to be determined by a complex interplay of RNA motifs and interacting proteins (7,8).

Recent evidence also points to a contribution of epigenetic marks and higher order chromatin structure to AS regulation (2). In support, genome-wide mapping has revealed enrichment of nucleosomes in exons (9,10) and several histone modifications are enriched in exons relative to intron (11). A mechanistic role for chromatin in AS is suggested by the finding that the histone acetyltransferase Gcn5 in yeast, and STAGA in humans, bind U2 snRNA, a component of the spliceosome (12). Histone acetylation is generally associated with euchromatin and is thought to stimulate RNA polymerase II (RNA pol II) elongation, which has been suggested to affect AS outcome (2,13). In support, switching promoters (14) and introduction of RNA pol II pause sites alters AS of select genes (15). Furthermore, chromatin features may directly affect splicing outcome by physical coupling of chromatin and the transcription machinery with the splicing apparatus via chromatin-binding adaptor proteins, which recognize alternatively spliced regions of genes enriched in particular histone modifications, and in turn recruit splicing regulators to the nascent RNA (2). A paradigm for such adaptor systems is the FGFR2 gene in which H3K36me3 is enriched over its alternatively spliced region (16). The modification is recognized by the epigenetic reader protein MRG15, which recruits the FGFR2 splicing regulator PTB to promote exon skipping (16). The

*To whom correspondence should be addressed. Tel: +301 496 8348; Fax: +301 496 4951; Email: maayan.salton@gmail.com
Correspondence may also be addressed to Tom Misteli. Tel: +301 402 3959; Fax: +301 496 4951; Email: mistelit@mail.nih.gov

level of H3K36me3 in the alternatively spliced region of FGFR2 appears to be regulated by Akt signaling pathways, suggesting that chromatin-mediated splicing regulation is a controlled physiological event (17). Similarly, Psip1/Ledgf binds H3K36me3 in various genes and alters AS outcome by recruitment of regulatory splicing factor SRSF1 and U5 snRNA (18). Another example for an adaptor system is the histone modification H3K4me3 in the *cyclin D1* gene, where the chromatin remodeler CHD1 binds H3K4me3 and recruits U2 snRNP (19). The interplay between chromatin and splicing may be bi-directional since splicing factors have been shown to recruit Setd2, the methyltransferase of H3K36 (20). These observations point to a prominent, yet poorly understood, regulatory role of chromatin features in AS control.

In order to identify additional chromatin regulators of AS, we used a cell-based *in vivo* assay for high-throughput screening of an siRNA chromatin library of 395 chromatin proteins. We identified 10 chromatin proteins with a role in AS regulation. As expected, the majority of these proteins have known roles in transcription. However, genome-wide analysis of transcription and AS changes after knockdown shows very limited overlap in affected genes, suggesting independent roles for these chromatin proteins in transcription and AS. To delineate the mechanistic basis of the cross-talk of transcription and AS, we focused on the H3K9 methyltransferase EHMT2. We show a distinct role for EHMT2 in transcription and AS of the VEGFA gene and we describe a novel chromatin-splicing adaptor system comprised of the heterochromatin protein 1γ (HP1γ), which recognizes H3K9me and recruits the splicing factor SRSF1. We identify H3K9me/HP1γ/SRSF1 as a major regulatory system of AS of the VEGFA gene.

MATERIALS AND METHODS

Cell lines and plasmids

U2OS (ATCC Number: HTB-96), HEK293 (ATCC Number: CRL-1573) and MCF7 (ATCC Number: HTB-22) cells were grown in Dulbecco's modified Eagle's medium supplemented with 10% fetal bovine serum; HUVEC (Human Umbilical Vein Endothelial Cells, ATCC Number: CRL-1730) cells were grown in F-12K medium containing 0.1 mg/ml heparin and 0.03 mg/ml endothelial cell growth supplement with 10% fetal bovine serum; all cell lines were maintained at 37°C and 5% CO_2 atmosphere. Cells were transfected with X-tremeGENE HP DNA Transfection Reagent (Roche) following the manufacturer's instructions. After 24 h in culture, transfected cells were used for experimentation. BIX01294 (Sigma) was used in 1 μM concentration for 24 h. Cells were exposed to hypoxic conditions in a chamber with a gas mixture of 94.5% N_2, 5% CO_2 and 0.5% O_2. The Tau reporter (pFlare5AdP-Tau10b) was provided by Dr P. Stoilov, School of Medicine, West Virginia University, USA; GFP-HP1γ was described by us before (21); and ZFP-EHMT2 and ZFP-No were provided by Sangamo BioSciences Inc (22).

siRNA transfection

Cells were transfected in triplicate on different days with siRNA oligos at a final concentration of 50 nM in a reverse format using a Janus automated liquid handler (Perkin-Elmer). First, 3.75 μl of OPTIMEM (Invitrogen) were transferred into each well of an empty PE-Cell Carrier 384-well imaging plate (Perkin-Elmer). Then, 1.25 μl of a 1 μM siRNA stock in OPTIMEM were added. Next, 5 μl of diluted Dharmafect1 were added. Plates were incubated 20 min at room temperature (RT) and then 5000 cells/well were seeded in the plate in a 15-μl volume of growing media, using a Multidrop Combi automated dispenser (ThermoFisher Scientific). Cells were analyzed after 72 h.

Automated imaging

Cells were fixed by adding 4% paraformaldehyde in phosphate buffered saline (PBS) directly into the culture medium and incubated for 15 min at RT. Cells were then washed 3× in PBS and stained with DRAQ5 (Biostatus Limited) 1:5, 000 in PBS. The automated imaging steps were performed using an Opera system (Perkin Elmer). Images were taken using a 488/640 nm excitation laser (1st acquisition) and a 568 nm excitation laser (2nd acquisition). Images were analyzed using the Acapella software package (Perkin-Elmer). The Green/Red ratio was calculated as the ratio between the average nuclear intensity signal in the 488 nm channel and the average nuclear signal in the 568 nm channel.

Statistical analysis

The Z'-score is routinely used in high-throughput screening to measure the power of an assay. Taking into account all assay measurements in a dataset including positive and negative controls, it measures the extent of distribution of individual sample responses in the assay and compares sample distribution to random distribution (23). A Z'-score between 0.5 and 1 is considered a high-quality assay. The Z-score defines the distance of a datapoint from the mean, taking into account all population parameters. Normalized Z-score values for the Green/Red ratio and the siRNA rank were calculated using the CellHTS2 package (24). siRNA pools with Z-score ≤ -3 were selected for secondary validation.

siRNA transfection of cells in a 96-well format

For the validation screen cells were transfected in duplicate on independent days with siRNA oligos at a final concentration of 50 nM in a reverse format. First, 15 μl of OPTIMEM (Invitrogen) were transferred into each well of an empty PE-CellCarrier 96-well imaging plate (Perkin-Elmer). Then, 5 μl of a 1-μM siRNA stock in OPTIMEM were added. Finally, 20 μl of diluted Dharmafect1 were added. Plates were incubated for 20 min at RT and ∼15, 000 cells/well were seeded in each well in a 60-μl volume of growing media. Every experiment was done in duplicate plates to allow for analysis after 72 h by both imaging and quantitative reverse transcriptase-polymerase chain reaction (qRT-PCR). RNA extraction, cDNA synthesis and qRT-PCR were performed using the Cells-To-Ct kit (Ambion) according to the manufacturer's instructions.

RNAi

siGenome pools and OnTargetPlus pools of four siRNA oligos per gene and OnTarget Plus SMART pool against EHMT1/2, EP300, PCAF, JunD, SAFB1, HP1γ and SRSF1 were purchased from Dharmacon. In experiments following the primary screen cells were grown to 20–50% confluence and transfected with siRNA using the DharmaFECT 1 reagent.

qRT-PCR

RNA was isolated from cells using the RNeasy plus mini kit (Qiagen). cDNA synthesis was carried out with the High Capacity cDNA Reverse Transcription Kit (Applied Biosystems). qPCR was performed with the SsoFast EvaGreen Supermix (BioRad) on the Biorad iCycler. The comparative Ct method was employed to quantify transcripts, and delta Ct was measured in triplicate. Primers used in this study are provided in Supplementary Table S5.

Chromatin immunoprecipitation

Approximately $2*10^6$ cells per sample were cross-linked for 15 min in 1% formaldehyde at RT. Cells were washed twice with cold PBS and lysed with lysis buffer (0.5% sodium dodecyl sulphate (SDS), 10 mM ethylenediaminetetraacetic acid (EDTA), 50 mM Tris–HCl pH8 and 1×protease inhibitor cocktail). DNA was sonicated in an ultrasonic bath (Bioruptor Diagenode) to an average length of 200–1000 bp. Supernatants were immunoprecipitated o/n with 40 μl of pre-coated anti-IgG magnetic beads (Dynabeads M-280 Invitrogen) previously incubated with the antibody of interest for 6 h at 4°C. The antibodies used were: mouse anti-HP1γ (3 μl, Chemicon MAB3450), mouse anti-H3K9me2 (3 μl, Abcam ab1220), EP300 (5 μl, Bethyl A300-358A), JunD (5 μl, Active Motif 39328), ERα (5 μl, Santa Cruz SC-543), SAFB1 (4 μl, provided by Steffi Oesterreich, University of Pittsburgh), ARID1B (3 μl, Abcam ab50958), SUV39H2 (20 μl, Abcam ab5264), EHMT2 (5 μl, Millipore 07-551). Control immunoprecipitations were performed with no antibody and H3K9me2 was normalized to anti-histone H3 chromatin immunoprecipitation (ChIP) (2 μl, Abcam ab1791). Beads were washed sequentially for 5 min each in Low-salt (20 mM Tris–HCl pH 8, 150 mM NaCl, 2 mM EDTA, 1% Triton X-100, 0.1% SDS), High-Salt (20 mM Tris–HCl pH 8, 500 mM NaCl, 2 mM EDTA, 1% Triton X-100, 0.1% SDS) and LiCl buffer (10 mM Tris pH 8.0, 1 mM EDTA, 250 mM LiCl, 1% NP-40, 1% Na-deoxycholate) and in Tris-EDTA (TE). Beads were eluted in 1% SDS and 100 mM $NaHCO_3$ buffer for 15 min at 65°C and cross-linking was reversed for 6 h after addition of NaCl to a final concentration of 200 mM and sequentially treated with 20 μg proteinase K. DNA was extracted using phenol chloroform. Immunoprecipitated DNA (2 out of 50 μl) and serial dilutions of the 10% input DNA (1:5, 1:25, 1:125 and 1:625) were analyzed by SYBR-Green real-time qPCR. ChIP-qPCR data were analyzed relative to input to include normalization for both background levels and the amount of input chromatin to be used in ChIP. The oligonucleotide sequences used are listed in Supplementary Table S5.

RNA-ChIP

RNA-ChIP was performed using the RNA-ChIP IT kit (Active Motif) according to the manufacturer's instructions with a few modifications. Protein G magnetic beads were pre-coated with anti-SRSF1 (50 μl, Santa Cruz SC-10254) for 2 h in RT. DNA was sonicated in an ultrasonic bath (Bioruptor Diagenode) for 11 cycles of 15 s ON and 30 s OFF. Serial dilutions of the 10% input DNA (1:5, 1:25, 1:125) were analyzed by SYBR-Green real-time qPCR. The oligonucleotide sequences used are listed in Supplementary Table S5.

Immunoblotting and immunoprecipitation

For immunoblotting cells were harvested and lysed with RIPA lysis buffer, and the extracts were run on a 4–12% Bis-Tris gel and transferred onto a polyvinylidene difluoride membrane. For immunoprecipitation cells were washed twice with ice-cold PBS, harvested and lysed for 30 min on ice in 0.5% NP40, 150 mM NaCl, 50 Mm Tris pH7.5, and 2 mM $MgCl_2$ supplemented with protease inhibitor and Benzonase Nuclease (Sigma). Supernatants were collected after centrifugation at 21, 000 g for 20 min. Supernatants were immunoprecipitated for 2 h with 40 μl of pre-coated anti-IgG magnetic beads (Dynabeads M-280, Invitrogen) and the SRSF1 antibody (Invitrogen 32-4500) for 6 h at 4°C. Beads were washed sequentially for 5 min each in Low-salt, High-Salt and LiCl buffer (as described for ChIP). Beads were boiled in sample buffer and loaded onto the gel for analysis. The samples were subjected to standard immunoblotting analysis using polyvinylidene difluoride membranes and enhanced chemiluminescence.

Migration assay

Migration assay was performed in a 96-well format by seeding approximately 50, 000 cells into wells that were pre-inserted with stoppers to occlude the center of the wells (Platypus Technologies Oris™ Cell Migration Assay). HUVEC (CRL-1730) cells were seeded in migration wells, and stoppers were removed after 4 h. Cells were allowed to migrate overnight in conditioned MCF7 cells media from either siNT or siEHMT2-treated cells. Cells were stained with Calcein-AM (Invitrogen) for 30 min prior to quantitative fluorescence reading using a BioTek Synergy HT microplate reader with excitation/emission wavelengths set at 485/525 nm, respectively.

PacBio sequencing

Taking advantage of the single molecule long reads of the PacBio sequencing system (Pacific Biosciences), we sequenced more than 60, 000 single molecules of cDNA from both siRNA control and siEHMT2-treated cells. Circular-consensus (CCS) reads of single molecules were aligned to the VEGFA genomic DNA with BLAT and alternatively spliced isoforms were identified and quantified using a custom Perl script.

Microarray analysis

Total RNA was reverse transcribed, labeled and hybridized to the Affymetrix Glue Grant human transcriptome (GG-H) array following the GeneChip Eukaryotic Double Strand Whole Transcript Protocol. Array was scanned using Affymetrix GeneChip scanner 7G.

RESULTS

A targeted high-throughput RNAi screen to identify chromatin regulators of AS

We set out to identify chromatin proteins with a role in pre-mRNA AS. In order to measure pre-mRNA splicing in a living cell, we used an established dual color AS reporter consisting of TAU exon 10, flanked by two constitutive exons, introduced into a U2OS human osteosarcoma cell line (25). The level of inclusion of the alternatively spliced TAU exon 10 is indicated by the ratio of the fluorescent reporter proteins GFP and StrawberryRed (Figure 1a). To validate the system, we silenced TRA2B, a known TAU exon 10 splicing regulator (26) (Supplementary Figure S1a). As expected, knockdown of TRA2B (Supplementary Figure S1a) promoted exclusion of TAU exon 10 as indicated by qPCR (Supplementary Figure S1b) and an increase in GFP signal (Figure 1b). Note that a concomitant reduction in StrawberryRed fluorescence signal is not expected due to the very long half-life (4.6 days) of the StrawberryRed protein (27), which was primarily used as an indicator of cell viability in the screen (see 'Materials and Methods').

In order to identify novel chromatin proteins involving in AS regulation, we generated an siRNA library containing pools of four siRNA oligonucleotides to 395 human genes with known chromatin annotation based on Gene Ontology (28) (Supplementary Table S1). The screen was conducted in triplicate in a 384-well format by reverse-transfecting cells with siRNA oligos for 72 h, followed by fixation of cells, and imaging to determine the cellular GFP/StrawberryRed signal ratio for each RNAi pool (see 'Materials and Methods' for details). The approach was validated using the positive siTRA2B control and a negative siNon-targeting control, yielding a Z'-score of 0.91. Of the 395 siRNA pools, 20 had a Z-score ≤ -3, a standard cut-off in optical screens, and were considered positive hits (Figure 1c). Two of the 20 hits were cytotoxic and caused cell death and were eliminated (Supplementary Table S1). Hits were validated using pools of chemically distinct siRNAs and splicing outcome was measured by both imaging and qPCR using specific primers (Supplementary Table S2). Two genes (BRDT and RAN) resulted in low viability of cells following silencing and were eliminated (Supplementary Table S2). Ten of 16 original hits were validated in this secondary screen (ARID5A, EP300, PCAF, EHMT2, SUV39H2, SAFB1, JunD, HMGN4, SMCHD1 and SCMH1). ChIP experiments using available antibodies against six of these proteins confirmed four candidates (SAFB1, JunD, EHMT2, EP300) to directly bind the TAU reporter (Figure 1d). All proteins bound both to the transcription start site (TSS) and, albeit consistently more weakly, to the constitutively spliced exon 3 in the body of the TAU reporter gene (Figure 1d). Although all identified hits promote exclusion of TAU exon 10 and no hits were

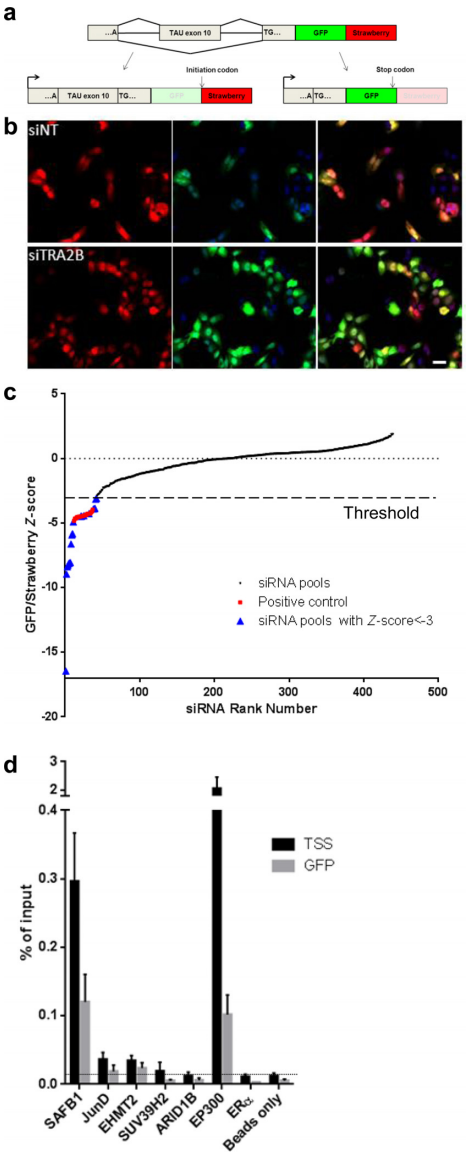

Figure 1. High-throughput imaging screen to identify chromatin proteins involved in AS regulation. (**a**) Schematic representation of the TAU reporter gene (25). Gray rectangles: exons, black lines: introns. The reporter consists of two external constitutive exons and a middle alternative exon 10 of the TAU gene. The translation initiation codon is split between the two constitutive exons resulting in GFP translation only following exclusion of the middle exon. In case of inclusion, a second initiation codon will be used to translate StrawberryRed. (**b**) U2OS cells stably expressing the TAU reporter gene were transfected with either siNon-Targeting (siNT) or siTRA2B and were grown in 384 well plates for 72 h. DRAQ5 stains the DNA and is used to identify the nuclei. Cells were fixed in paraformaldehyde and imaged sequentially at 488, 568 and 640 nm (20×magnification, 1 imaging field). Scale bar: 40 μm. (**c**) U2OS cells stably expressing the TAU reporter gene were screened in triplicate using a library containing 395 siRNA pools targeting human genes with a chromatin GO annotation. siRNA pools were ranked according to their Z-score in the GFP/StrawberryRed ratio when compared to the median value of the population. Positive control wells (red) were silenced for TRA2B. The horizontal broken line represents the threshold ($Z \leq -3$) used for selection of hits. (**d**) ChIP of the indicated protein along the TAU reporter in U2OS cells stably expressing the reporter. Transcription start site (TSS) was probed as was the GFP region of the reporter. ERα was used as a negative control based on its screen score. Horizontal broken line represents the threshold set by the beads only sample and ERα. Values represent averages of three independent experiments ±SD.

found to promote inclusion, this may be a technical bias in the assay due to the long half-life of StrawberryRed, making exclusion easier to detect.

Independent roles of chromatin factors in transcription and AS

The majority of hits identified as splicing regulators in the screen had previously been implicated in transcriptional control. To rule out that the observed effects on AS were a secondary consequence of transcriptional changes, we compared the effect of knockdown of candidate chromatin proteins on genome-wide transcription and AS. For this analysis we chose four chromatin proteins (EP300, EHMT2, JunD and SAFB1) that were positive in our screen and directly bind the TAU reporter (Figure 1d). PCAF was added to the analysis as a known interactor of EP300 (29). We used the Affymetrix Glue Grant human transcriptome (GG-H) array, which contains probes spanning exon-exon junctions to detect AS isoforms, as well as exon probes for general mRNA transcription levels, allowing for simultaneous mapping of transcripts and AS patterns on the same array using the same RNA samples (30). We analyzed the results using the Partek Genomics Suite (31) and JETTA (32) for transcripts and AS, respectively. Individual genes were silenced in MCF7 cells and analyzed in triplicates. Non-targeting oligos were used as control (Supplementary Figure S2a–e).

Knockdown of individual chromatin proteins affected the transcription level of between 62 (JunD) and 335 (EP300) genes (Figure 2). Correspondingly, between 81 (SAFB1) and 662 (PCAF) AS were affected. However, no correlation between the number of changes in transcript level and the number of AS changes was observed and while loss of some chromatin factors, such as EP300 and SAFB1, resulted in more transcript level changes than AS events, others such as JunD and PCAF affected AS more than transcription (Figure 2). Of note, with the exception of EHMT2, all factors showed an at least ∼2-fold preference for either affected transcript levels or AS, suggesting a preferential impact of each protein on either process (Figure 2). Remarkably, the number of genes in which both transcription and splicing were affected was minimal ranging from 2 (PCAF and JunD) to 10 (EP300) events (Figure 2a–e and Supplementary Table S3). Knockdown of the chromatin proteins did not affect expression of pre-mRNA splicing factors based on microarray analysis (Supplementary Figure S2f). These results suggest independent functions of chromatin proteins in transcription and AS regulation.

The histone methyltransferase EHMT2 regulates VEGFA AS

In order to understand the separate roles of chromatin modifiers in regulating transcription or AS in more detail, we sought to elucidate the mechanism of AS regulation for one of these chromatin proteins. We focused on EHMT2, a SET domain-containing histone lysine methyltransferase, predominantly found in a heterodimer with EHMT1 (33), which mono- and dimethylate Lys 9 in histone H3 (33,34). H3K9 methylation is associated with heterochromatin (35) and EHMT2 is considered a mediator of epigenetic gene silencing (36).

Knockdown analysis of EHMT2 identified VEGFA, a prominent cellular growth factor with major roles in various physiological processes including cell migration and angiogenesis, as an AS target of EHMT2 (Supplementary Table S3). In support of a regulatory role in AS of VEGFA, EHMT2 bound to the intragenic region of VEGFA (Supplementary Figure S3a). As such we used VEGFA as a model system to delineate its mechanism of action. VEGFA is a signaling protein produced mainly by endothelial cells and is involved in stimulating angiogenesis (37). Numerous VEGFA isoforms have been described, although their functional roles are poorly characterized (38–41). The major splicing isoforms are $VEGFA_{121}$, $VEGFA_{165}$ and $VEGFA_{189}$, each expressed as an a- and b-isoform generated in a combinatorial fashion by usage of alternate exons 8a or 8b (Figure 3a). As previously reported (42), MCF7 cells have comparable levels of $VEGFA_{121}$ and $VEGFA_{165}$, and lower amounts of $VEGFA_{189}$ (Supplementary Figure S3b). As observed in our microarray analysis, knockdown of EHMT2 by siRNA did not alter the total transcript level of VEGFA when measured by qPCR (Figure 3b). In order to get a full picture of the VEGFA splicing isoform abundance following EHMT2 silencing, we enriched for VEGFA isoforms using primers in exon 3 and the 3′ UTR and sequenced VEGFA isoforms using PacBio sequencing (Supplementary Table S4; see 'Materials and Methods'). Compared to a siNT sample, the number of sequencing reads in the siEHMT2 sample was the same for $VEGFA_{121}$, but was reduced by∼20% for $VEGFA_{189}$, and the $VEGFA_{165}$ isoform was only detected in the siEHMT2 sample, indicating activation of a new AS event upon EHMT2 silencing (Supplementary Table S4). Read numbers were skewed toward $VEGFA_{121}$ due to a bias in the template-to-product ratio toward the shorter isoform generated during multitemplate PCR amplification prior to sequencing. Using junction primers to identify specific VEGFA isoforms, we did not find any effect of EHMT2 loss on isoforms $VEGFA_{121}$a/b, whereas $VEGFA_{165}$a/b increased and $VEGFA_{189}$a/b decreased (Supplementary Figure S3c). This pattern of splicing suggests that EHMT2 promotes inclusion of exon 6a (Figure 3a). The effect of EHMT2 silencing on VEGFA exon 6a exclusion was confirmed since similar results were observed using the EHMT2 inhibitor BIX01294 (43) and after silencing of EHMT1 (Supplementary Figure S3d), the heterodimer partner of EHMT2 (33) (Figure 3b and c). We conclude that loss of EHMT1/2 does not alter VEGFA transcription but affects its AS.

Recruitment of EHMT2 to its target gene mediates AS regulation

To demonstrate that EHMT2 recruitment and methylation of H3K9 were functionally important for VEGFA splicing, we created H3K9me2 marks on VEGFA in a controlled fashion by taking advantage of a fusion protein between a Zn-Finger protein (ZFP), recognizing the promoter of VEGFA, and the minimal catalytic domain of EHMT2 (22). This construct tethers EHMT2 to the VEGFA promoter and has previously been shown to increase H3K9me2 locally and to repress transcription of VEGFA in HEK293 cells (22). As expected, when teth-

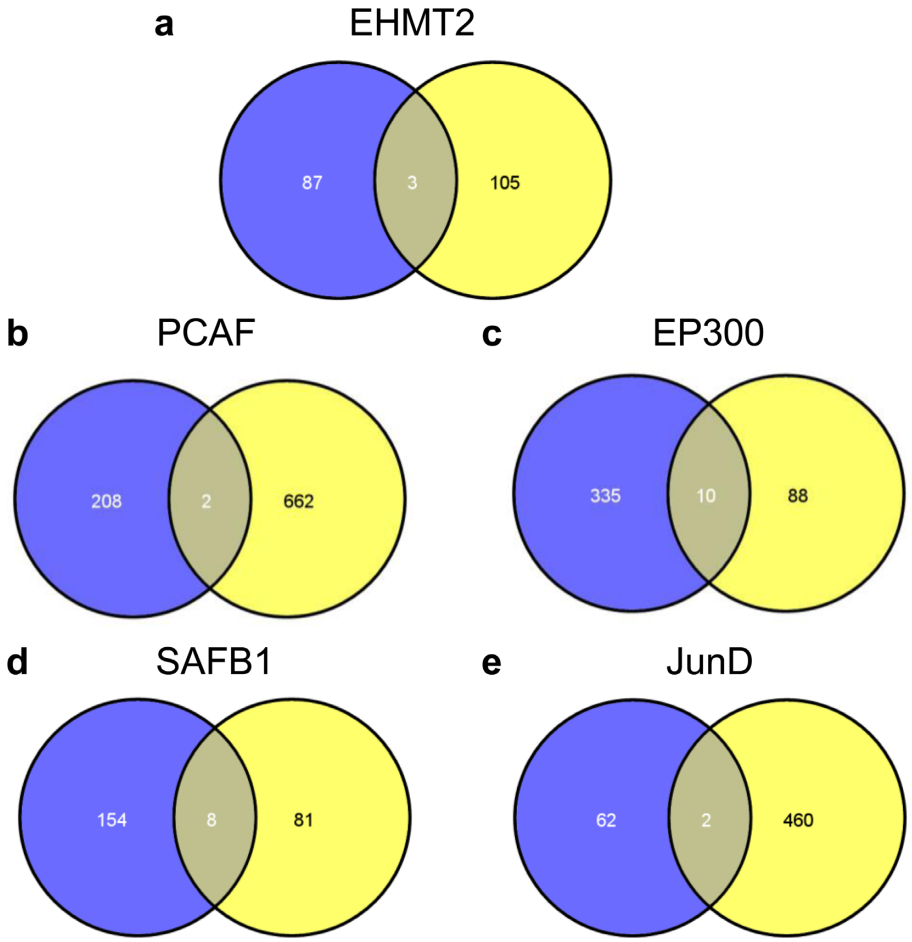

Figure 2. Independent role of chromatin factors in transcription and AS. MCF7 cells were transfected with siNT, siEHMT2 (**a**), siPCAF (**b**), siEP300 (**c**), siSAFB1 (**d**) or siJunD (**e**) for 72 h. Total RNA was extracted and analyzed on a GG-H array. Venn diagram representing total RNA levels (blue) and AS events (yellow) is presented for each of the genes. The detailed gene list is in Supplementary Table S4.

ered to VEGFA in HEK293 cells, EHMT2 reduced VEGFA mRNA levels (Figure 3d). Regardless, at the same time VEGFA exon 6a inclusion was enhanced (Figure 3e). In contrast, no effect was seen on $VEGFA_{121}$, which is not sensitive to EHMT2 levels (Figure 3e). ChIP for H3K9me2 following tethering of EHMT2 to VEGFA promoter confirmed enrichment of the modification in the promoter as well as spreading to the intragenic region (Figure 3f). We conclude that the local concentration of H3K9me2 at the VEGFA promoter is sufficient to regulate AS of exon 6a in VEGFA.

The HP1γ acts as a splicing adaptor

Histone modifications over alternatively spliced gene regions have previously been shown to act as recognition sites for epigenetic adaptor proteins, which in turn recruit splicing factors (2). The H3K9me modification created by EHMT2 is a recognition site for HP1γ (44–46). ChIP analysis in MCF7 cells shows HP1γ binding to the alternatively spliced exon 6a region, intron 7 and the 3′ intragenic region, but not the promoter of the VEGFA gene (Figure 4a). Binding to these sites was reduced following treatment with BIX01294, an inhibitor of EHMT2 (Figure 4a). On the other hand, ChIP for HP1γ following tethering of EHMT2 to the VEGFA promoter revealed higher occupancy of HP1γ in the promoter region as well as the intragenic regions (Figure 4b), demonstrating recruitment of HP1γ to VEGFA upon binding of EHMT2. To test whether HP1γ has an effect on VEGFA splicing outcome, HP1γ was silenced using siRNA. Loss of HP1γ resulted in exclusion of exon 6a (Figure 4c and Supplementary Figure S4a), whereas overexpression of HP1γ promoted its inclusion (Figure 4c). These observations suggest a pivotal role for HP1γ in VEGFA AS. In contrast to a genome-wide study showing that loss of HP1γ promotes intron retention (47), silencing of HP1γ did not promote retention of introns 5 and 7 in the alternatively spliced region of VEGFA (Supplementary Figure S4b).

To test whether EHMT2 and HP1γ act in the same regulatory pathway or exerted their effects independently, we tethered EHMT2 to the VEGFA promoter and silenced HP1γ at the same time. While tethering of EHMT2 in the presence of HP1γ promotes exon 6a inclusion (Figure 4d), tethered EHMT2 failed to activate VEGFA exon 6a splicing in the absence of HP1γ (Figure 4d). In contrast, knockdown of HP1γ did not reverse the inhibitory effect of tethering of EHMT2 on VEGFA total mRNA levels, suggest-

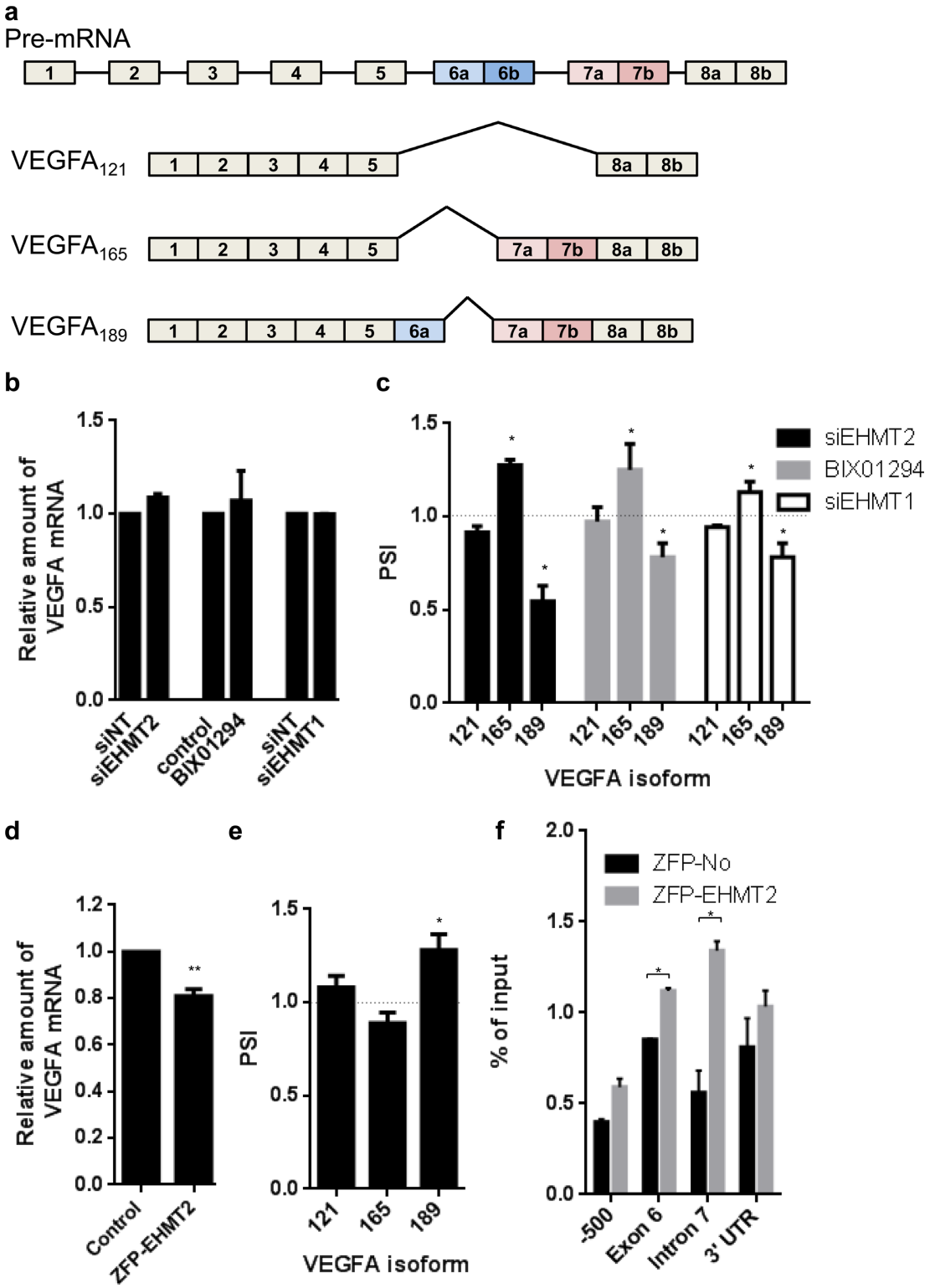

Figure 3. EHMT2 promotes inclusion of VEGFA exon 6a. (**a**) Schematic representation of the VEGFA gene and three of its known isoforms. Rectangles: exons, black lines: introns. (**b** and **c**) MCF7 cells were transfected with siNT, siEHMT2 or siEHMT1 for 72 h or treated with BIX01294 for 24 h. mRNA levels were assessed using qPCR; VEGFA mRNA amount is normalized to the housekeeping gene *cyclophillin A* or (c) VEGFA isoform values normalized to total VEGFA mRNA. Results are presented as proportion of splicing isoform (PSI), indicating the amount of the isoform relative to the total amount of VEGFA mRNA. Horizontal broken lines indicate siNT control values. (**d**–**f**). HEK293 cells were transfected with either ZFP-No (ZFP binding domain alone) or ZFP-EHMT2 for 24 h. mRNA levels were assessed using qPCR; VEGFA mRNA amount was normalized to the housekeeping gene *cyclophillin A* or (e) VEGFA isoform values normalized to total VEGFA mRNA; dashed line indicates ZFP-No control values. (f) ChIP of H3K9me2 along the VEGFA gene. The percentage of input was normalized to unmodified H3. Values represent means ± SEM from three independent experiments. (a–f) Values represent averages of three independent experiments ± SD (*$P < 0.05$, **$P < 0.01$, *t*-test).

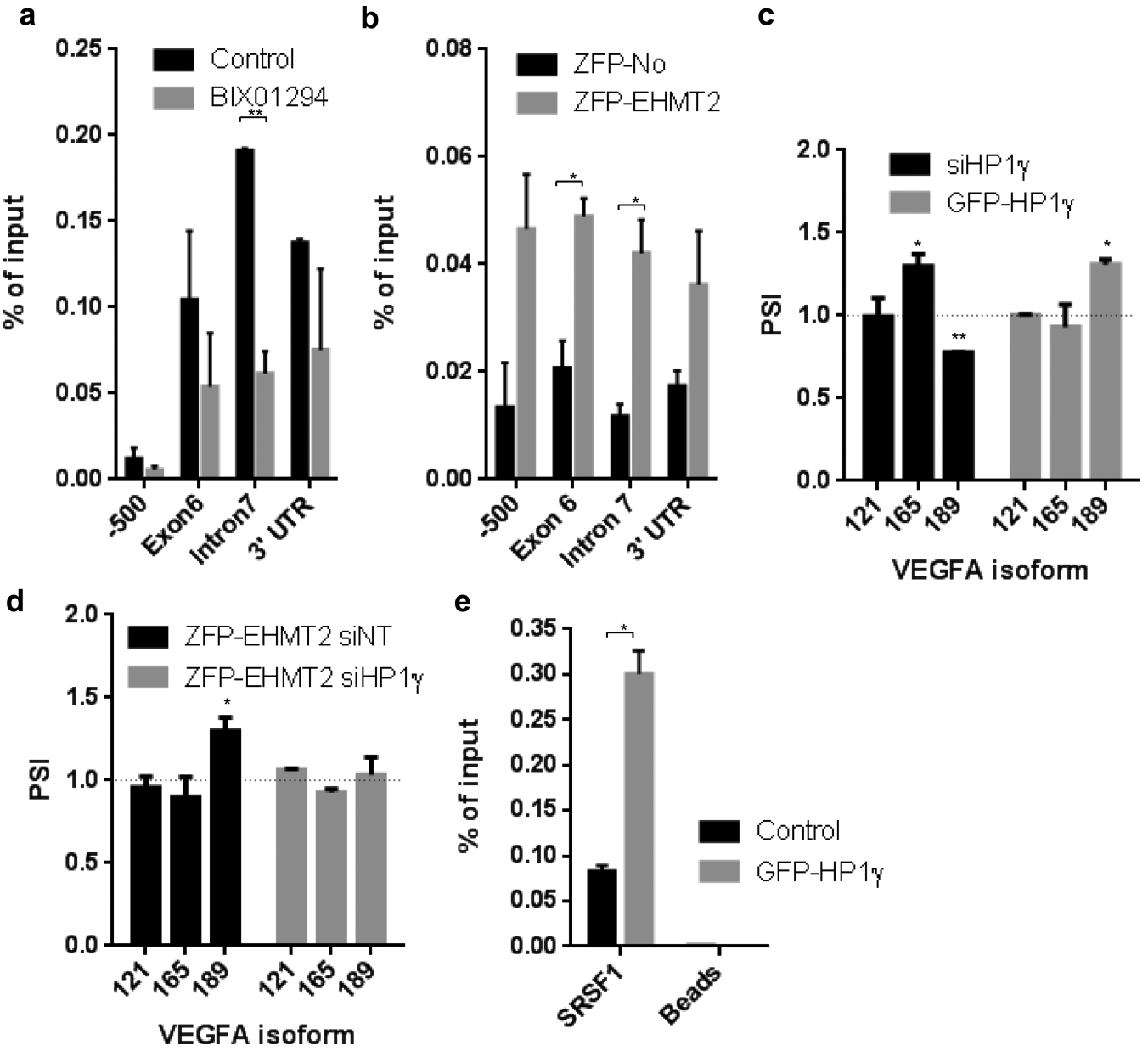

Figure 4. An H3K9me/HP1γ/SRSF1 adaptor system on *VEGFA*. (**a**) ChIP of HP1γ along VEGFA in MCF7 cells treated with BIX01294 for 24 h. (**b**) ChIP of HP1γ along VEGFA in HEK293 cells transfected with either ZFP-No (ZFP binding domain alone) or ZFP-EHMT2 for 24 h. (**c**) MCF7 cells were transfected with siNT or siHP1γ for 72 h or HEK293 cells were transfected with either GFP-empty vector or GFP-HP1γ for 24 h. mRNA levels were assessed using qPCR; VEGFA isoform values are normalized to total VEGFA mRNA; dashed line indicates siNT of GFP-empty vector values. (**d**) HEK293 cells were transfected with siNT or siHP1γ for 48 h and then transfected with ZFP-No or ZFP-EHMT2 for 24 h. mRNA levels were assessed using qPCR; VEGFA isoform values are normalized to total VEGFA mRNA; dashed line indicates ZFP-No/siNT values or ZFP-No/siHP1γ. (**e**) RNA-ChIP of SRSF1 to VEGFA mRNA in HEK293 cells transfected with either GFP-empty vector or GFP-HP1γ for 24 h. (a, b, e) Values represent means ± SEM from three independent experiments. (c and d) Values represent averages of three independent experiments ±SD (*$P < 0.05$, **$P < 0.01$, *t*-test).

ing that HP1γ is not necessary for regulation of VEGFA transcription by EHMTs (Supplementary Figure S4c), further demonstrating the independent, and mechanistically distinct, functions of EHMT2 on transcription and splicing.

Recruitment of SRSF1 by HP1γ modulates VEGFA splicing

The splicing factor SRSF1 is a known regulator of VEGFA AS (48). Silencing of SRSF1 in MCF7 cells promotes exclusion of exon 6a, mimicking the effect of EHMT1/2 and HP1γ (Supplementary Figure S4d). One possibility is that these proteins cooperate in AS regulation of VEGFA. In order to test this hypothesis, we probed for physical interaction of HP1γ and SRSF1 in HEK293 cells. Immunoprecipitation using specific antibodies against the endogenous proteins demonstrated physical interaction of SRSF1 with HP1γ (Supplementary Figure S4e), pointing to the presence of these two proteins in the same complex. To probe

if HP1γ contributes to the recruitment of SRSF1 to the VEGFA pre-mRNA, we performed RNA-ChIP for SRSF1 following either silencing or overexpression of HP1γ. Overexpressing HP1γ led to approximately three times more SRSF1 binding to VEGFA mRNA (Figure 4e), and silencing had the opposite effect (Supplementary Figure S4f). Overexpression or silencing of HP1γ did not affect SRSF1 mRNA levels (Supplementary Figures S4g and S4h).

Since we had originally identified EHMT2 as an AS regulator of the TAU reporter gene, we asked whether the H3K9me/HP1γ/SRSF1 system also acts on the endogenous TAU gene. Silencing of EHMT2 in MCF7 cells had no effect on total TAU mRNA levels (Supplementary Figure S4i). However, silencing of EHMT2, HP1γ or SRSF1 all promoted exclusion of TAU exon10 (Supplementary Figure S4j). The effect of EHMT2 was local since, TAU exon 10 AS was not affected when EHMT2 was tethered to the VEGFA promoter (Supplementary Figure S4k).

Hypoxia-induced VEGFA AS regulation is mediated by EHMT2

EHMT2 protein levels increase in response to hypoxia (49–53) and total VEGFA is strongly upregulated following hypoxia to promote angiogenesis (54). To probe for potential physiological relevance of the observed AS regulation via EHMT2, we analyzed VEGFA splicing under hypoxic conditions. As previously reported, exposure of MCF7 cells to hypoxia for 6 h resulted in a moderate increase in EHMT2 and an about 2–3-fold increase in VEGFA mRNAs (Supplementary Figure S5a). Concomitantly, hypoxia resulted in increased inclusion of VEGFA exon 6a (Figure 5a), similar to that observed upon tethering of EHMT2 (Figure 3e). Importantly, hypoxia-induced VEGFA exon 6a inclusion was sensitive to the EHMT2 catalytic inhibitor BIX01294, demonstrating that this effect was due to changes in H3K9me levels (Figure 5a). We conclude that hypoxia-induced changes in AS of VEGFA are dependent on EHMT2.

To finally demonstrate physiological relevance of EHMT2-mediated AS of VEGFA, we investigated whether silencing of EHMT2 affects endothelial migration via altering the VEGFA splicing isoform repertoire. Since VEGFA isoforms are secreted proteins, we collected media from MCF7 cells silenced for EHMT2 and used it to assess endothelial cell migration, which is dependent on VEGFA isoforms (Supplementary Figure S5b). Silencing of EHMT2 resulted in an ∼20% induction of $VEGFA_{165}$ and an almost 50% reduction of $VEGFA_{189}$ compared to control cells (siNT). These changes in VEGFA splicing isoforms were accompanied by an ∼2.5-fold reduction of migration of endothelial cells (Figure 5b). We conclude that loss of EHMT2 affects VEGFA splicing to decrease endothelial cell migration.

DISCUSSION

We have here used a high-throughput screen to identify chromatin modifiers of AS. We describe several novel chromatin proteins that regulate AS. Not surprisingly, the vast majority of chromatin-based splicing modulators are known transcriptional regulators. RNA splicing is thought to occur co-transcriptionally (55) and there is extensive evidence for coupling of the two processes both kinetically and via physical interaction of the RNA splicing machinery with RNA polymerase (1). In particular, the C-terminal domain (CTD) of RNA pol II has been implicated in splicing factor recruitment (3). However, using genome-wide comparative expression and AS analysis, we show that the identified chromatin proteins act independently on transcription and AS. The differential effects on the two processes are likely due to the location of the modifications. While promoter modifications are likely to contribute to transcriptional control, intragenic methylated H3K9 may recruit splicing factors to alternatively spliced regions in the body of the gene, as previously demonstrated by genome wide-mapping and biochemical approaches (56–61). In line with this interpretation, we identify the H3K9me-binding protein HP1γ as an adaptor protein that promotes recruitment of the VEGFA splicing regulator SRSF1. Further support for this interpretation is the observation that tethering of EHMT2 to the VEGFA promoter reduces its transcriptional activity, but promotes exon 6a inclusion concomitantly with the spreading of H3K9 methylation from the tethered region upstream of the TSS to the 3′ intragenic region including the alternatively spliced region of VEGFA. It is of note, that the effect of EHMT2 tethering is functionally distinct from loss of EHMT2, which does not affect transcription, but only modulates splicing. This observation suggests that EHMT2 is not necessary for the maintenance of the transcriptional status of VEGFA, but is needed to maintain the VEGFA splicing pattern. The observed requirement for a histone modification in the maintenance of a particular splicing pattern is similar to that observed for H3K36me3 in the FGFR2 gene (16). It is also of note, that silencing of HP1γ, the adaptor for H3K9me2, while tethering EHMT2 to the VEGFA promoter abolishes the AS effect, but has no effect on reduced transcription of VEGFA by EHMT2 (Figure 4d and Supplementary Figure S4c), suggesting that the inhibitory effect of EHMT2 on transcription does not involve HP1γ, but likely another epigenetic reader.

The identification of EHMT2 in an AS screen points to an unanticipated regulatory role for EHMT2 in alternative pre-mRNA splicing. Previous work has linked H3K9me3 to AS of CD44 (59) and NCAM (61). Consistent with this observation, we also detected CD44 AS changes in response to silencing of EHMT2 in our genome-wide analysis (Supplementary Table S3), whereas NCAM was not expressed in the MCF7 cells analyzed here. We identified an adaptor complex consisting of H3K9me/HP1γ/SRSF1 as a regulator of VEGFA exon 6a splicing. While previous work provided evidence for regulation of AS of CD44 by H3K9me3 via pausing of RNA pol II, the reported effects of HP1γ (59) and SRSF1 (62) on AS of CD44 may suggest the involvement of a H3K9me/HP1γ/SRSF1 adaptor complex as a complementary mechanism in CD44 splicing. Our results furthermore show that elevated levels of methylated H3K9 in the body of the VEGFA gene promote exon 6a inclusion, promoting formation of $VEGFA_{189}$ in favor of $VEGFA_{165}$. Increased production of $VEGFA_{165}$ by EHMT2 was previously described in airway smooth muscle cells in asthma (63) and attributed to transcription regula-

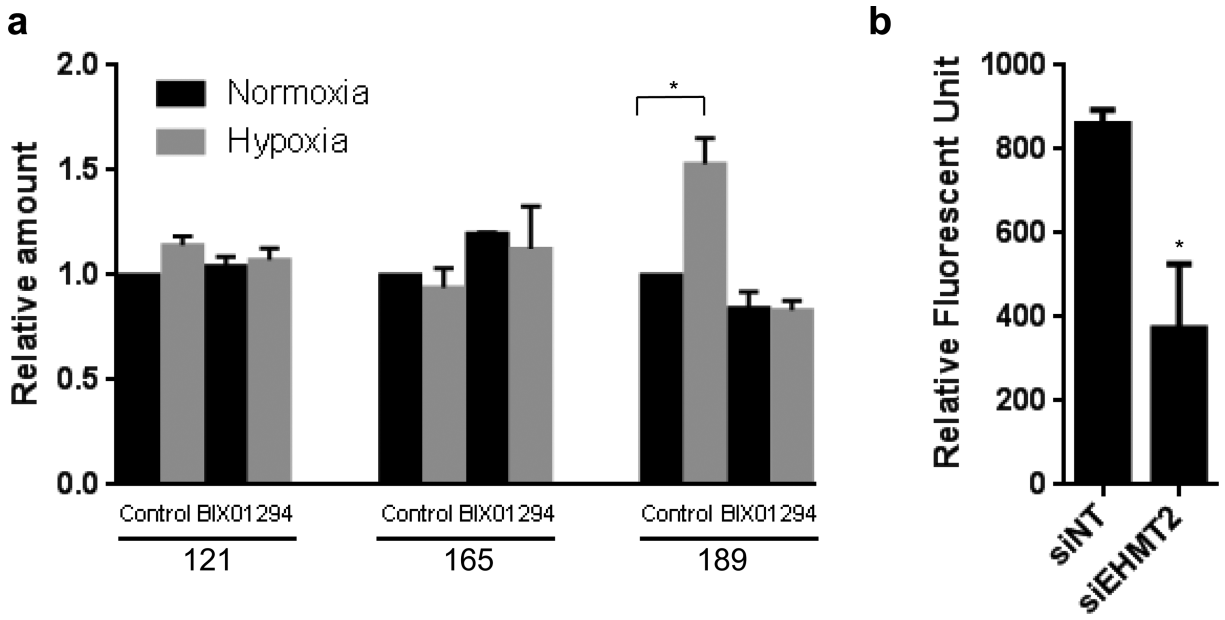

Figure 5. Hypoxia induced inclusion of VEGFA exon 6a in *EHMT2*-dependent manner. (**a**) Hypoxia was induced for 6 h in MCF7 cells treated with BIX01294 for 24 h. mRNA levels were assessed using qPCR; VEGFA isoform values are normalized to total VEGFA mRNA. (**b**) MCF7 cells were transfected with siNT or siEHMT2. Conditioned cell culture medium collected after 72 h was used in Oris^{TM} Cell Migration Assay to monitor the migration of endothelial HUVEC cells. Cells were stained with Calcein AM to determine the degree of cell migration using fluorescent units. (a and b) Values represent averages of two independent experiments each with three repeats ±SD (*$P < 0.05$, **$P < 0.01$, *t*-test).

tion. We suggest here a distinct mechanism for EHMT2 in promoting $VEGFA_{165}$ isoform.

EHMT2-mediated AS regulation appears to be of physiological relevance. Previous work has demonstrated induction of EHMT2 in response to environmental changes such as lack of oxygen (49–53). Our results expand these findings by demonstrating a direct role of EHMT2 in AS regulation of VEGFA via recruitment of SRSF1. We show that altering the isoform abundance of VEGFA by EHMT2 is pro-angiogenic. In line with our results, SRSF1 has previously been shown to have a pro-angiogenic effect (64). Thus, induction of EHMT2 following hypoxia is expected to change VEGFA isoform repertoire in line with promoting angiogenesis. Taken together, our results provide further evidence for a regulatory role of chromatin in RNA processing. While transcription and RNA splicing are closely coupled, our findings suggest that chromatin factors independently affect transcription and RNA processing. Based on the recent finding of regulation of AS of FGFR2 via AKT signaling through a splicing adaptor system (17), and our current observations on hypoxia, it seems likely that these inter-related regulatory mechanisms will be of significant relevance in physiological and pathological processes.

SUPPLEMENTARY DATA

Supplementary Data are available at NAR Online.

ACKNOWLEDGMENTS

We thank Reini Luco, Paola Scaffidi and Shalini Oberdoerffer for helpful discussions, Peter Stoilov for TAU dual color reporter gene, Sangamo BioSciences Inc. for ZFP-EHMT2, Steffi Oesterreich for advice and SAFB1 antibody, Guy Morgenstern for help with microarray analysis, Xu Xiaolin for help with PacBio analysis, Martin Playford for help with the BioTek microplate reader. This work was in part performed at the NCI High-Throughput Imaging Facility.

FUNDING

Intramural Research Program of the National Institutes of Health (NIH), NCI, Center for Cancer Research. Funding for open access charge: NIH Intramural Program.
Conflict of interest statement. None declared.

REFERENCES

1. Maniatis,T. and Reed,R. (2002) An extensive network of coupling among gene expression machines. *Nature*, **416**, 499–506.
2. Luco,R.F., Allo,M., Schor,I.E., Kornblihtt,A.R. and Misteli,T. (2011) Epigenetics in alternative pre-mRNA splicing. *Cell*, **144**, 16–26.
3. Bentley,D.L. (2014) Coupling mRNA processing with transcription in time and space. *Nat. Rev. Genet.*, **15**, 163–175.
4. Graveley,B.R. (2001) Alternative splicing: increasing diversity in the proteomic world. *Trends Genet.*, **17**, 100–107.
5. Pan,Q., Shai,O., Lee,L.J., Frey,B.J. and Blencowe,B.J. (2008) Deep surveying of alternative splicing complexity in the human transcriptome by high-throughput sequencing. *Nat. Genet.*, **40**, 1413–1415.
6. Wang,E.T., Sandberg,R., Luo,S., Khrebtukova,I., Zhang,L., Mayr,C., Kingsmore,S.F., Schroth,G.P. and Burge,C.B. (2008) Alternative isoform regulation in human tissue transcriptomes. *Nature*, **456**, 470–476.
7. Barash,Y., Calarco,J.A., Gao,W., Pan,Q., Wang,X., Shai,O., Blencowe,B.J. and Frey,B.J. (2010) Deciphering the splicing code. *Nature*, **465**, 53–59.
8. Irimia,M. and Blencowe,B.J. (2012) Alternative splicing: decoding an expansive regulatory layer. *Curr. Opin. Cell Biol.*, **24**, 323–332.

9. Schwartz,S., Meshorer,E. and Ast,G. (2009) Chromatin organization marks exon-intron structure. *Nat. Struct. Mol. Biol.*, **16**, 990–995.
10. Andersson,R., Enroth,S., Rada-Iglesias,A., Wadelius,C. and Komorowski,J. (2009) Nucleosomes are well positioned in exons and carry characteristic histone modifications. *Genome Res.*, **19**, 1732–1741.
11. Zhou,H.L., Luo,G., Wise,J.A. and Lou,H. (2014) Regulation of alternative splicing by local histone modifications: potential roles for RNA-guided mechanisms. *Nucleic Acids Res.*, **42**, 701–713.
12. Gunderson,F.Q. and Johnson,T.L. (2009) Acetylation by the transcriptional coactivator Gcn5 plays a novel role in co-transcriptional spliceosome assembly. *PLoS Genet.*, **5**, e1000682.
13. Kornblihtt,A.R., Schor,I.E., Allo,M., Dujardin,G., Petrillo,E. and Munoz,M.J. (2013) Alternative splicing: a pivotal step between eukaryotic transcription and translation. *Nat. Rev. Mol. Cell Biol.*, **14**, 153–165.
14. Cramer,P., Pesce,C.G., Baralle,F.E. and Kornblihtt,A.R. (1997) Functional association between promoter structure and transcript alternative splicing. *Proc. Natl Acad. Sci. U.S.A.*, **94**, 11456–11460.
15. Roberts,G.C., Gooding,C., Mak,H.Y., Proudfoot,N.J. and Smith,C.W. (1998) Co-transcriptional commitment to alternative splice site selection. *Nucleic Acids Res.*, **26**, 5568–5572.
16. Luco,R.F., Pan,Q., Tominaga,K., Blencowe,B.J., Pereira-Smith,O.M. and Misteli,T. (2010) Regulation of alternative splicing by histone modifications. *Science*, **327**, 996–1000.
17. Sanidas,I., Polytarchou,C., Hatziapostolou,M., Ezell,S.A., Kottakis,F., Hu,L., Guo,A., Xie,J., Comb,M.J., Iliopoulos,D. *et al.* (2014) Phosphoproteomics screen reveals akt isoform-specific signals linking RNA processing to lung cancer. *Mol. Cell*, **53**, 577–590.
18. Pradeepa,M.M., Sutherland,H.G., Ule,J., Grimes,G.R. and Bickmore,W.A. (2012) Psip1/Ledgf p52 binds methylated histone H3K36 and splicing factors and contributes to the regulation of alternative splicing. *PLoS Genet.*, **8**, e1002717.
19. Sims,R.J. III, Millhouse,S., Chen,C.F., Lewis,B.A., Erdjument-Bromage,H., Tempst,P., Manley,J.L. and Reinberg,D. (2007) Recognition of trimethylated histone H3 lysine 4 facilitates the recruitment of transcription postinitiation factors and pre-mRNA splicing. *Mol. Cell*, **28**, 665–676.
20. de Almeida,S.F., Grosso,A.R., Koch,F., Fenouil,R., Carvalho,S., Andrade,J., Levezinho,H., Gut,M., Eick,D., Gut,I. *et al.* (2011) Splicing enhances recruitment of methyltransferase HYPB/Setd2 and methylation of histone H3 Lys36. *Nat. Struct. Mol. Biol.*, **18**, 977–983.
21. Cheutin,T., McNairn,A.J., Jenuwein,T., Gilbert,D.M., Singh,P.B. and Misteli,T. (2003) Maintenance of stable heterochromatin domains by dynamic HP1 binding. *Science*, **299**, 721–725.
22. Snowden,A.W., Gregory,P.D., Case,C.C. and Pabo,C.O. (2002) Gene-specific targeting of H3K9 methylation is sufficient for initiating repression *in vivo*. *Curr. Biol.*, **12**, 2159–2166.
23. Birmingham,A., Selfors,L.M., Forster,T., Wrobel,D., Kennedy,C.J., Shanks,E., Santoyo-Lopez,J., Dunican,D.J., Long,A., Kelleher,D. *et al.* (2009) Statistical methods for analysis of high-throughput RNA interference screens. *Nat. Methods*, **6**, 569–575.
24. Boutros,M., Bras,L.P. and Huber,W. (2006) Analysis of cell-based RNAi screens. *Genome Biol.*, **7**, R66.
25. Stoilov,P., Lin,C.H., Damoiseaux,R., Nikolic,J. and Black,D.L. (2008) A high-throughput screening strategy identifies cardiotonic steroids as alternative splicing modulators. *Proc. Natl Acad. Sci. U.S.A.*, **105**, 11218–11223.
26. Jiang,Z., Tang,H., Havlioglu,N., Zhang,X., Stamm,S., Yan,R. and Wu,J.Y. (2003) Mutations in tau gene exon 10 associated with FTDP-17 alter the activity of an exonic splicing enhancer to interact with Tra2 beta. *J. Biol. Chem.*, **278**, 18997–19007.
27. Verkhusha,V.V., Kuznetsova,I.M., Stepanenko,O.V., Zaraisky,A.G., Shavlovsky,M.M., Turoverov,K.K. and Uversky,V.N. (2003) High stability of Discosoma DsRed as compared to Aequorea EGFP. *Biochemistry*, **42**, 7879–7884.
28. Ashburner,M., Ball,C.A., Blake,J.A., Botstein,D., Butler,H., Cherry,J.M., Davis,A.P., Dolinski,K., Dwight,S.S., Eppig,J.T. *et al.* (2000) Gene ontology: tool for the unification of biology. The Gene Ontology Consortium. *Nat. Genet.*, **25**, 25–29.
29. Song,C.Z., Keller,K., Murata,K., Asano,H. and Stamatoyannopoulos,G. (2002) Functional interaction between coactivators CBP/p300, PCAF, and transcription factor FKLF2. *J. Biol. Chem.*, **277**, 7029–7036.
30. Xu,W., Seok,J., Mindrinos,M.N., Schweitzer,A.C., Jiang,H., Wilhelmy,J., Clark,T.A., Kapur,K., Xing,Y., Faham,M. *et al.* (2011) Human transcriptome array for high-throughput clinical studies. *Proc. Natl Acad. Sci. U.S.A.*, **108**, 3707–3712.
31. Downey,T. (2006) Analysis of a multifactor microarray study using Partek genomics solution. *Methods Enzymol.*, **411**, 256–270.
32. Seok,J., Xu,W., Gao,H., Davis,R.W. and Xiao,W. (2012) JETTA: junction and exon toolkits for transcriptome analysis. *Bioinformatics*, **28**, 1274–1275.
33. Tachibana,M., Ueda,J., Fukuda,M., Takeda,N., Ohta,T., Iwanari,H., Sakihama,T., Kodama,T., Hamakubo,T. and Shinkai,Y. (2005) Histone methyltransferases G9a and GLP form heteromeric complexes and are both crucial for methylation of euchromatin at H3-K9. *Genes Dev.*, **19**, 815–826.
34. Shinkai,Y. and Tachibana,M. (2011) H3K9 methyltransferase G9a and the related molecule GLP. *Genes Dev.*, **25**, 781–788.
35. Nakayama,J., Rice,J.C., Strahl,B.D., Allis,C.D. and Grewal,S.I. (2001) Role of histone H3 lysine 9 methylation in epigenetic control of heterochromatin assembly. *Science*, **292**, 110–113.
36. Tachibana,M., Matsumura,Y., Fukuda,M., Kimura,H. and Shinkai,Y. (2008) G9a/GLP complexes independently mediate H3K9 and DNA methylation to silence transcription. *EMBO J.*, **27**, 2681–2690.
37. Ferrara,N., Gerber,H.P. and LeCouter,J. (2003) The biology of VEGF and its receptors. *Nat. Med.*, **9**, 669–676.
38. Carmeliet,P., Ng,Y.S., Nuyens,D., Theilmeier,G., Brusselmans,K., Cornelissen,I., Ehler,E., Kakkar,V.V., Stalmans,I., Mattot,V. *et al.* (1999) Impaired myocardial angiogenesis and ischemic cardiomyopathy in mice lacking the vascular endothelial growth factor isoforms VEGF164 and VEGF188. *Nat. Med.*, **5**, 495–502.
39. Zhang,H.T., Scott,P.A., Morbidelli,L., Peak,S., Moore,J., Turley,H., Harris,A.L., Ziche,M. and Bicknell,R. (2000) The 121 amino acid isoform of vascular endothelial growth factor is more strongly tumorigenic than other splice variants *in vivo*. *Br. J. Cancer*, **83**, 63–68.
40. Herve,M.A., Buteau-Lozano,H., Vassy,R., Bieche,I., Velasco,G., Pla,M., Perret,G., Mourah,S. and Perrot-Applanat,M. (2008) Overexpression of vascular endothelial growth factor 189 in breast cancer cells leads to delayed tumor uptake with dilated intratumoral vessels. *Am. J. Pathol.*, **172**, 167–178.
41. Grunstein,J., Masbad,J.J., Hickey,R., Giordano,F. and Johnson,R.S. (2000) Isoforms of vascular endothelial growth factor act in a coordinate fashion To recruit and expand tumor vasculature. *Mol. Cell. Biol.*, **20**, 7282–7291.
42. Mineur,P., Colige,A.C., Deroanne,C.F., Dubail,J., Kesteloot,F., Habraken,Y., Noel,A., Voo,S., Waltenberger,J., Lapiere,C.M. *et al.* (2007) Newly identified biologically active and proteolysis-resistant VEGF-A isoform VEGF111 is induced by genotoxic agents. *J. Cell Biol.*, **179**, 1261–1273.
43. Kubicek,S., O'Sullivan,R.J., August,E.M., Hickey,E.R., Zhang,Q., Teodoro,M.L., Rea,S., Mechtler,K., Kowalski,J.A., Homon,C.A. *et al.* (2007) Reversal of H3K9me2 by a small-molecule inhibitor for the G9a histone methyltransferase. *Mol. Cell*, **25**, 473–481.
44. Bannister,A.J., Zegerman,P., Partridge,J.F., Miska,E.A., Thomas,J.O., Allshire,R.C. and Kouzarides,T. (2001) Selective recognition of methylated lysine 9 on histone H3 by the HP1 chromo domain. *Nature*, **410**, 120–124.
45. Lachner,M., O'Carroll,D., Rea,S., Mechtler,K. and Jenuwein,T. (2001) Methylation of histone H3 lysine 9 creates a binding site for HP1 proteins. *Nature*, **410**, 116–120.
46. Canzio,D., Larson,A. and Narlikar,G.J. (2014) Mechanisms of functional promiscuity by HP1 proteins. *Trends Cell Biol.*, **24**, 377–386.
47. Smallwood,A., Hon,G.C., Jin,F., Henry,R.E., Espinosa,J.M. and Ren,B. (2012) CBX3 regulates efficient RNA processing genome-wide. *Genome Res.*, **22**, 1426–1436.
48. Nowak,D.G., Woolard,J., Amin,E.M., Konopatskaya,O., Saleem,M.A., Churchill,A.J., Ladomery,M.R., Harper,S.J. and Bates,D.O. (2008) Expression of pro- and anti-angiogenic isoforms of VEGF is differentially regulated by splicing and growth factors. *J. Cell Sci.*, **121**, 3487–3495.
49. Lee,J.S., Kim,Y., Kim,I.S., Kim,B., Choi,H.J., Lee,J.M., Shin,H.J., Kim,J.H., Kim,J.Y., Seo,S.B. *et al.* (2010) Negative regulation of hypoxic responses via induced Reptin methylation. *Mol. Cell*, **39**, 71–85.

50. Wang,Z., Yang,D., Zhang,X., Li,T., Li,J., Tang,Y. and Le,W. (2011) Hypoxia-induced down-regulation of neprilysin by histone modification in mouse primary cortical and hippocampal neurons. *PLoS One*, **6**, e19229.
51. Chen,H., Yan,Y., Davidson,T.L., Shinkai,Y. and Costa,M. (2006) Hypoxic stress induces dimethylated histone H3 lysine 9 through histone methyltransferase G9a in mammalian cells. *Cancer Res.*, **66**, 9009–9016.
52. Lee,S.H., Kim,J., Kim,W.H. and Lee,Y.M. (2009) Hypoxic silencing of tumor suppressor RUNX3 by histone modification in gastric cancer cells. *Oncogene*, **28**, 184–194.
53. Lee,J.S., Kim,Y., Bhin,J., Shin,H.J., Nam,H.J., Lee,S.H., Yoon,J.B., Binda,O., Gozani,O., Hwang,D. *et al.* (2011) Hypoxia-induced methylation of a pontin chromatin remodeling factor. *Proc. Natl Acad. Sci. U.S.A.*, **108**, 13510–13515.
54. Arcondeguy,T., Lacazette,E., Millevoi,S., Prats,H. and Touriol,C. (2013) VEGF-A mRNA processing, stability and translation: a paradigm for intricate regulation of gene expression at the post-transcriptional level. *Nucleic Acids Res.*, **41**, 7997–8010.
55. Brody,Y. and Shav-Tal,Y. (2011) Transcription and splicing: when the twain meet. *Transcription*, **2**, 216–220.
56. Spies,N., Nielsen,C.B., Padgett,R.A. and Burge,C.B. (2009) Biased chromatin signatures around polyadenylation sites and exons. *Mol. Cell*, **36**, 245–254.
57. Dhami,P., Saffrey,P., Bruce,A.W., Dillon,S.C., Chiang,K., Bonhoure,N., Koch,C.M., Bye,J., James,K., Foad,N.S. *et al.* (2010) Complex exon-intron marking by histone modifications is not determined solely by nucleosome distribution. *PLoS One*, **5**, e12339.
58. Allo,M., Buggiano,V., Fededa,J.P., Petrillo,E., Schor,I., de la Mata,M., Agirre,E., Plass,M., Eyras,E., Elela,S.A. *et al.* (2009) Control of alternative splicing through siRNA-mediated transcriptional gene silencing. *Nat. Struct. Mol. Biol.*, **16**, 717–724.
59. Saint-Andre,V., Batsche,E., Rachez,C. and Muchardt,C. (2011) Histone H3 lysine 9 trimethylation and HP1gamma favor inclusion of alternative exons. *Nat. Struct. Mol. Biol.*, **18**, 337–344.
60. Hon,G., Wang,W. and Ren,B. (2009) Discovery and annotation of functional chromatin signatures in the human genome. *PLoS Comput. Biol.*, **5**, e1000566.
61. Schor,I.E., Fiszbein,A., Petrillo,E. and Kornblihtt,A.R. (2013) Intragenic epigenetic changes modulate NCAM alternative splicing in neuronal differentiation. *EMBO J.*, **32**, 2264–2274.
62. Galiana-Arnoux,D., Lejeune,F., Gesnel,M.C., Stevenin,J., Breathnach,R. and Del Gatto-Konczak,F. (2003) The CD44 alternative v9 exon contains a splicing enhancer responsive to the SR proteins 9G8, ASF/SF2, and SRp20. *J. Biol. Chem.*, **278**, 32943–32953.
63. Clifford,R.L., John,A.E., Brightling,C.E. and Knox,A.J. (2012) Abnormal histone methylation is responsible for increased vascular endothelial growth factor 165a secretion from airway smooth muscle cells in asthma. *J. Immunol.*, **189**, 819–831.
64. Blanco,F.J. and Bernabeu,C. (2012) The Splicing Factor SRSF1 as a Marker for Endothelial Senescence. *Front. Physiol.*, **3**, 54.